ELSEVIER

Ceramics International 31 (2005) 215–222

CERAMICS INTERNATIONAL

www.elsevier.com/locate/ceramint

Development of red wall tiles by the dry process using Brazilian raw materials

S.J.G. Sousa, J.N.F. Holanda*

Advanced Materials Laboratory, Northern Fluminense State University, Campos dos Goytacazes-RJ 28013-602, Brazil

Received 6 February 2004; received in revised form 8 March 2004; accepted 19 May 2004
Available online 25 August 2004

Abstract

This work presents the results of a study concerning the processing of red wall tile composed of clay, calcareous, and quartz from Brazil. The formulation prepared by dry process was optimized depicting the effect of the calcareous addition (12–18 mass%) on the densification behaviour during the firing process. The samples were unidirectionally dry pressed in a die with rectangular cavity and fired in air at temperatures ranging from 1080 to 1200 °C using a fast-firing cycle. The samples were characterized before and after firing. The development of the microstructure was followed by XRD and SEM. The densification was measured by three parameters: linear shrinkage, water absorption, and flexural strength. The results revealed that the red wall tile bodies containing abundant calcareous fired above 1000 °C form gehlenite and anorthite. Moreover, the densification behaviour was found to be influenced by the calcareous content and sintering temperature. The microstructure is constituted of a network of small dense zones interconnected with a porous phase. It was also found that the requirements specified in the Brazilian tile standards concerning the BIII class tiles were fulfilled, depending on calcareous content and sintering temperature.

Keywords: A. Sintering; B. Microstructure-final; C. Strength; Tiles

1. Introduction

Ceramic wall tiles are a multicomponent system primarily composed of clay, carbonates, and quartz, and is considered to be one of the most complex ceramic materials. Each component within the body contributes differently to the final properties. The formulations of wall tiles also can be referred to as triaxial wall tiles [1]. On sintering, the triaxial wall tiles system forms a mixture of glass and crystalline phases depending upon the chemical compositions of the raw materials and processing conditions. Most of the reactions occurring during sintering are kinetically governed processes that do not reach thermodynamic equilibrium. This occurs due to the fact that single fast-firing cycles as short as 1 h have been widely employed [2]. In addition, the crystalline phases formed are responsible for important properties of the wall tiles such as high dimensional stability (low linear shrinkage), low hidratability, and high porosity [3].

Brazil is currently the fourth word-wide producer and exporter of ceramic floor and wall tiles [4]. The evolution of the Brazilian tile production (wall and floor tiles) is shown in Fig. 1 [5]. As can be observed, the Brazilian ceramic wall and floor industry has presented a rapid growth since 1993. In 2001, Brazilian tile industry grow around 4.5% with production of 473.4 million meter square. In addition, the Brazilian production can grow still more due the high internal demand and opportunities for growth of the exportations.

Although there is a great commercial interest in wall tiles, very little research has been conducted in Brazil in developing of wall tile [6]. Within this context, the present paper discusses, in detail, the processing of wall tile using ceramic raw materials from Campos-RJ (Brazil). These raw materials have not been tested for wall tiles yet. Thus, the inves-

* Corresponding author. Tel.: +55 22 2726 1623; fax: +55 22 2726 1533.
E-mail address: holanda@uenf.br (J.N.F. Holanda).

0272-8842/$30.00 © 2004 Published by Elsevier Ltd and Techna Group S.r.l.
doi:10.1016/j.ceramint.2004.05.003

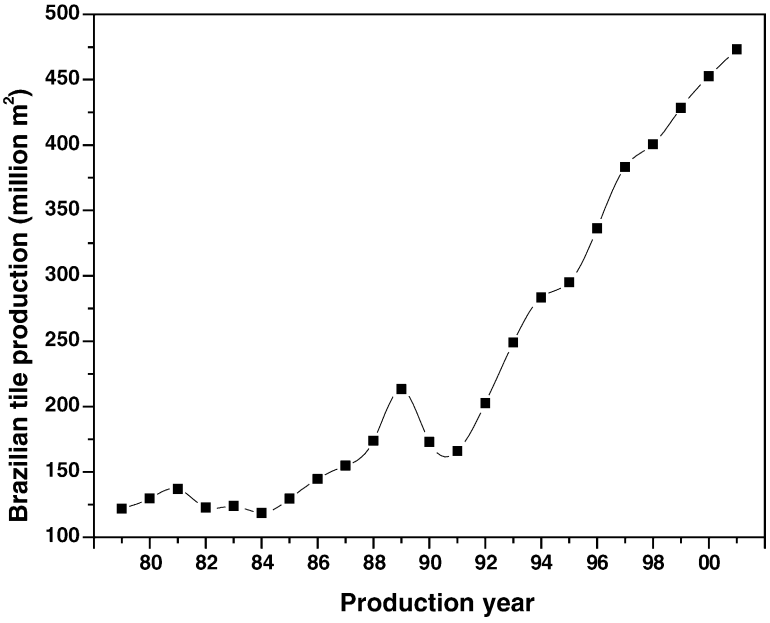

Fig. 1. Evolution of the Brazilian wall and floor tiles production.

tigation of the their use for manufacturing of red wall tile bodies is of high interest from an academic and technological viewpoint.

In the present study, three red wall tile compositions were formulated, using raw materials from Campos-RJ, Brazil. The densification behaviour of these three compositions was investigated. Emphasis is given to the formulation characteristics, their effects on the physical–mechanical properties of the end product, and the microstructure evolution of the pressed specimens during densification.

2. Experimental procedure

Red wall tile compositions were formulated (Table 1) using clay–calcareous–quartz mixtures with calcareous additions up to 18 wt.%. Clay and calcareous are from the area around Campos-RJ (Brazil), which has a large ceramic industry. It was used a commercial quartz. Table 2 gives the chemical compositions of the raw materials.

The different steps involved in the dry granulation process are shown schematically in Fig. 2. The granulation process of the ceramic formulations was performed by three distinct operations: grinding, mixing, and agglomeration. The raw materials were dry-ground and mixing using a laboratory mill, with a screening residue of 4%, on screens with 63 μm net openings (250 mesh). The samples of dry-ground powders were homogenized and granulated in a high intensity mixer (Eirich, type RO2) with moisture content of 14% (moisture mass/dry mass). After reducing the moisture content to 7%, the granules were kept in a dissecator for 24 h to homogenize their moisture content. The granulated powder is sent to the sieve to eliminate agglomerates larger than 2 mm.

The ceramic formulations prepared were characterized by X-ray diffraction (URD-65 Diffractometer, Seifert), using monochromatic Cu Kα radiation. Scanning speed was set to 1.5° (2θ)/min. The phases were identified from peak positions and intensities using reference data from the JCPDS handbook [7]. TG/DTG were carried out with a TA Instruments SDT-2960 Simultaneous TG-DTA on the powder samples, under air atmosphere from room temperature

Table 1
Ceramic formulations (mass%)

Raw materials	Number		
	M1	M2	M3
Clay	70	70	70
Calcareous	12	15	18
Quartz	18	15	12

Table 2
Chemical compositions of the raw materials (mass%)

Compounds	Raw materials		
	Clay	Calcareous	Quartz
SiO_2	46.42	6.01	99.66
Al_2O_3	27.90	0.81	0.15
Fe_2O_3	9.10	0.55	0.04
CaO	0.22	47.26	–
MgO	0.71	4.91	–
MnO	0.11	0.01	–
TiO_2	1.32	0.06	0.01
Na_2O	0.36	0.15	–
K_2O	1.67	0.23	–
P_2O_5	0.21	0.07	–
LOI[a]	11.96	39.94	0.25

[a] LOI, loss on ignition.

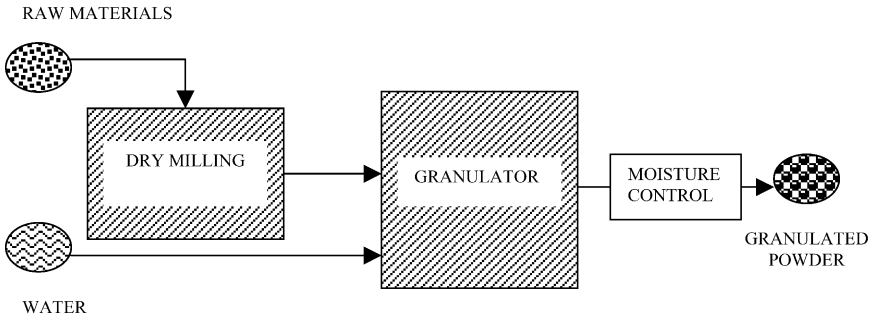

Fig. 2. Outline of the dry granulation process.

up to 1150 °C at a heating rate of 10 °C/min. The granule-size distribution of the granulated powders was determined by procedures according to NBR 7181-84. The morphology and the surface topography of the granules were observed by scanning electron microscopy (SEM).

Specimens were prepared by uniaxial pressing technique in a 11.5 cm × 2.5 cm rectangular die at 35 MPa, and dried at 110 °C. The firing step was carried out in a fast-firing laboratory kiln at temperatures varying from 1080 to 1200 °C for a fast-firing cycle of total 60 min including cooling.

The densification behaviour was described in terms of linear shrinkage, water absorption, and flexural strength. Linear shrinkage values upon drying and firing were evaluated from the variation of the length of the rectangular specimens. Water absorption values were determined from weight differences between the as-fired and water saturated samples (immersed in boiling water for 2 h). The flexural strength was determined by three-point bending test (model 1125, Instron) at a loading rate of 0.5 mm/min according to the NBR 9451 standard.

The sintered microstructure of the samples was observed by scanning electron microscopy (DSM 962, Zeiss), where the accelerating voltage was kept constant at 10 kV. Electrical charging was avoided by gold coating on the specimens. The phase identification of the sintered specimens was performed at room temperature by X-ray diffractometry.

3. Results and discussion

The XRD patterns of the ceramic formulations are shown in Fig. 3. Apart from kaolinite phase, characteristic peaks of quartz, gibbsite, and calcite were identified. Furthermore, there are small amounts of mica muscovite and dolomite. It was also observed that the peak intensities are influenced by the ceramic formulation.

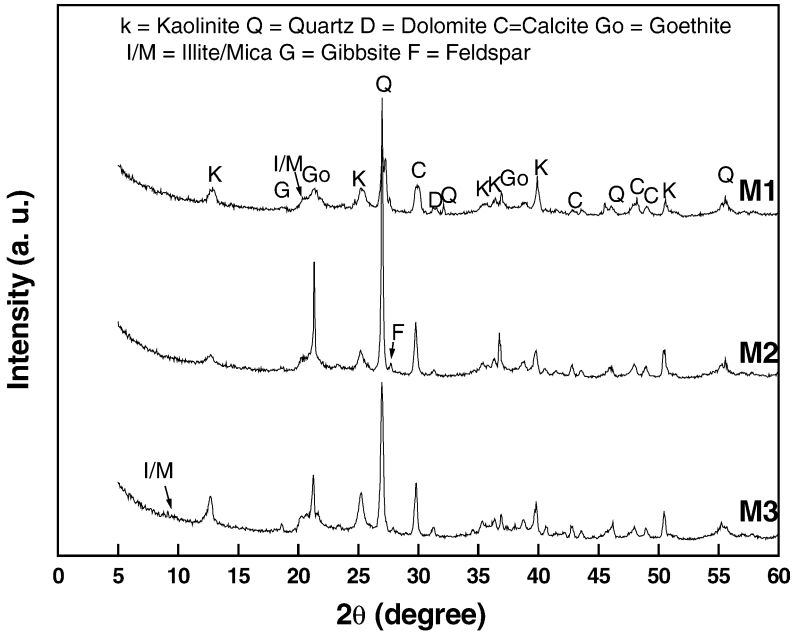

Fig. 3. X-ray diffraction patterns for the ceramic formulations.

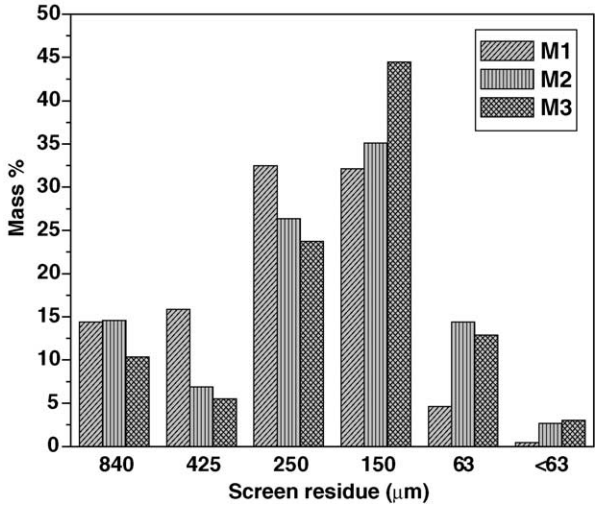

Fig. 4. Grain-size distribution of granulated powders produced by the dry process.

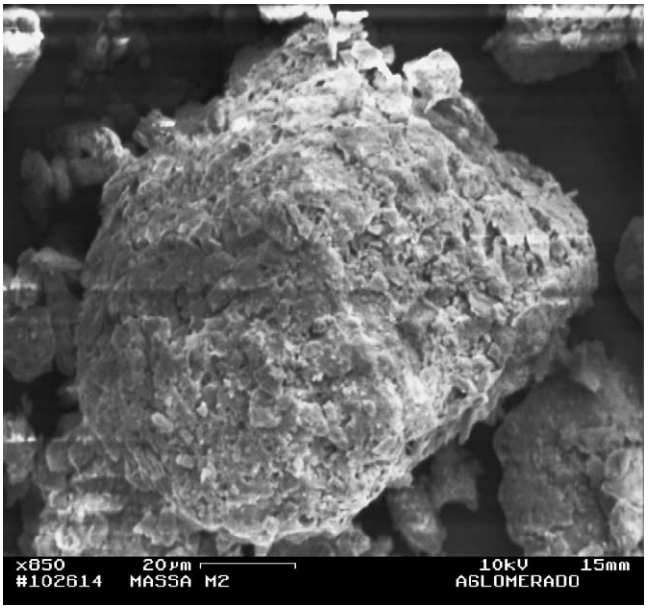

Fig. 5. Granulated powder for porous wall tile.

Table 3
Properties of the specimens in the dried state

Ceramic formulation	Drying properties		
	Apparent density (g cm^{-3})	Linear shrinkage (%)	Flexural strength (MPa)
M1	1.90 ± 0.01	0.04 ± 0.01	3.44 ± 0.38
M2	1.91 ± 0.01	0.04 ± 0.03	4.11 ± 0.68
M3	1.90 ± 0.01	0.05 ± 0.03	3.35 ± 0.57

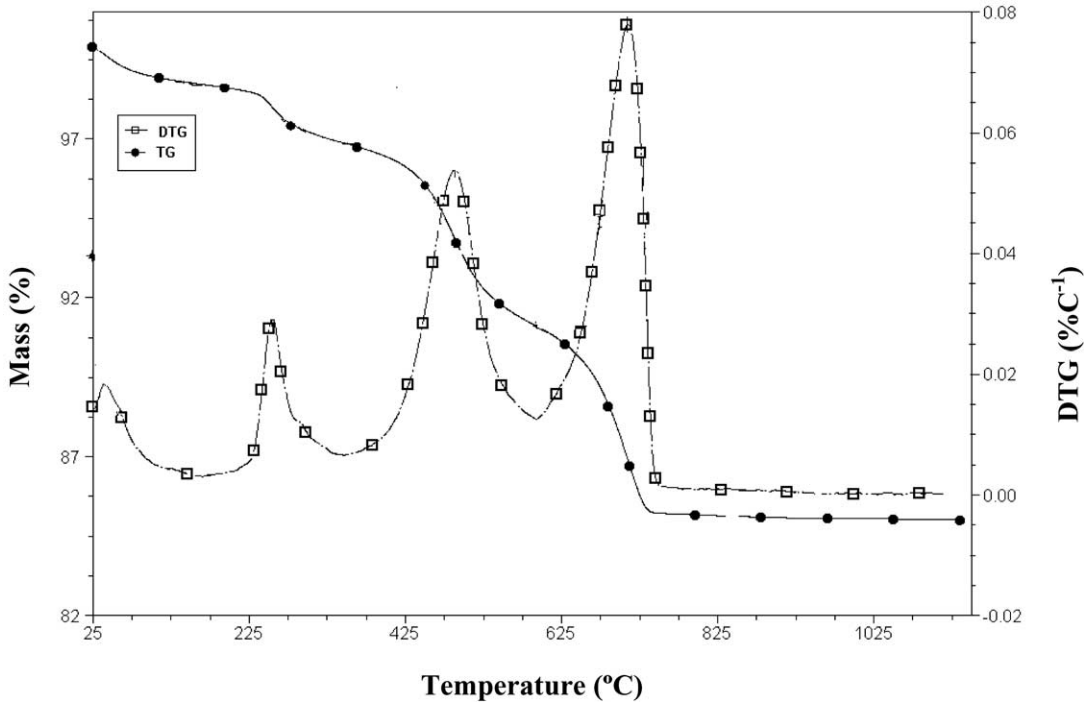

Fig. 6. TG–DTG curves for the ceramic formulation M2.

The grain-size distribution of the granulated powders produced by dry process is shown in Fig. 4. The results revealed that the calcareous addition modified the grain-size distribution. The largest fraction of the granulated powder M1 is in the grain-size range of 250–425 μm. The granulated powders M2 and M3 presented largest fraction in the grain-size range of 150–250 μm. However, the predominance of larger size grains for all granulated powders are within the intermediate grain range adequate to obtain good reactivity during firing of the powders produced with the dry process [8]. In addition, these granulated powders exhibited efficient flow rate that is important to automatic die filling during the compaction step. The scanning electron micrograph of Fig. 5 shows the shape and surface features of granulated powders (formulation M2). The irregular shape is typical of powders produced by mechanical agglomeration of finely dry-ground particles. These observations hold for all the prepared ceramic formulations.

The TG/DTG curves for the ceramic formulation M2 are shown in Fig. 6. Four weight loss events are seen in the TG and DTG curves, in sequence as temperature rises. These events can be mainly interpreted as the release of free moisture, dehydration of hydroxides mainly gibbsite, dehydroxylation of kaolinite, and carbonates decomposition (calcite and dolomite), respectively. The samples presented a total weight loss during the heating within the 13.72–16.96% range. The higher in the amount of calcareous, the greater the weight loss is observed.

The properties of the specimens in the dried state are presented in Table 3. The results demonstrate that no significant differences in the drying density of the specimens were observed among the prepared ceramic bodies. This is very important because all specimens are about the same density so as to make a comparison of fired properties and densification. In addition, the values of drying density of the specimens (1.90–1.91 g/cm^3) are within the limits for the industrial production of wall tiles [9]. In the drying step, it is adequate to obtain a value of linear shrinkage between 0 and 0.3% in order to avoid cracks, fissures, and warpage [10]. Thus, the linear shrinkage for all ceramic bodies satisfies the recommended limits. It was also observed that the specimens presented drying flexural strength between 3.35 and 4.11 MPa, being acceptable according to the literature [10] that requires values higher than 2.5 MPa.

Densification was monitored through the gresification diagram, which corresponds to the simultaneous variation of the linear shrinkage and water absorption as a function of the sintering temperature. This diagram is of crucial importance to understanding of the effects of calcareous addition on the densification of wall tile bodies. Fig. 7(a)–(c) show the gresification diagrams of the sintered bodies. It is clear that the densification depends substantially on both calcareous content and maximum firing temperature. The gradual increase of the calcareous content (12–18 wt.%) tends to retard the densification during sintering. The presence of calcium carbonate ($CaCO_3$) modifies the reactions course

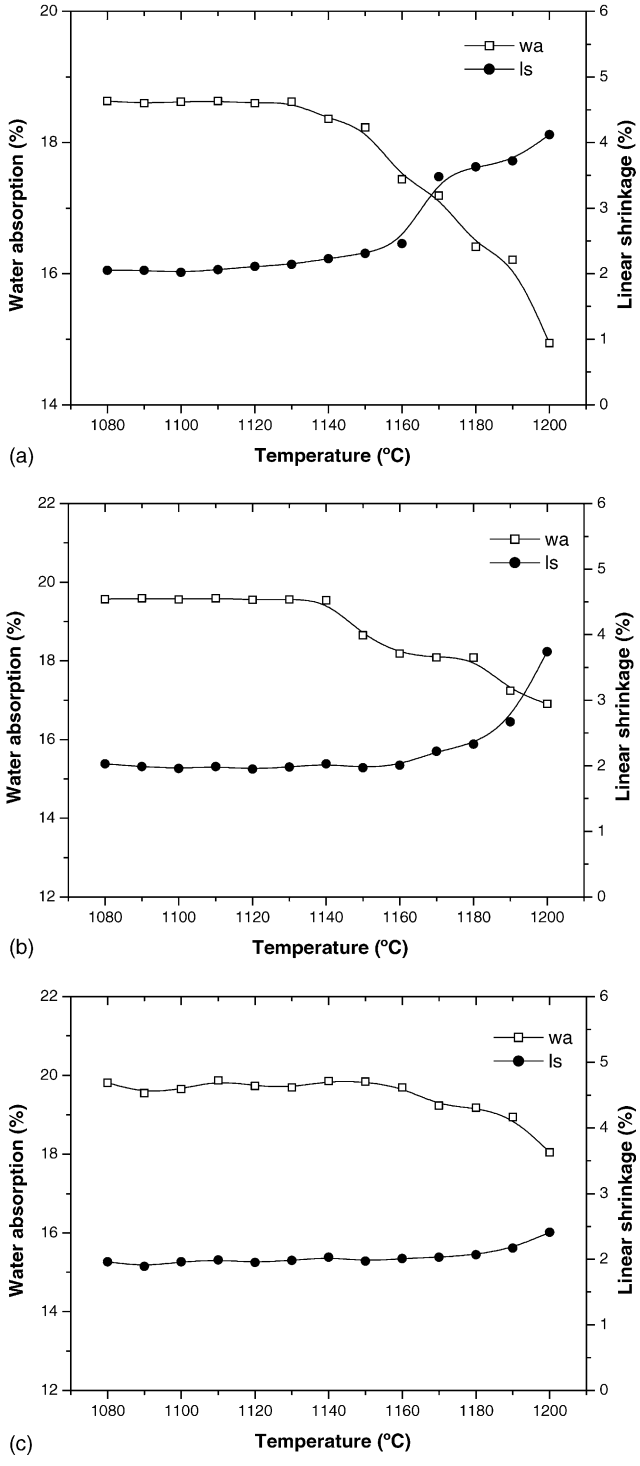

Fig. 7. Gresification diagram of the sintered bodies: (a) M1; (b) M2; and (c) M3.

and affects the formation of the liquid phase [11]. During preheating, between 800 and 900 °C, the $CaCO_3$ decomposes to CaO accompanied by the evolution of CO_2 outside the structure of fired bodies. The CaO reacts with the amorphous phase (metakaolinite), which quickly diminishes at increasing firing temperature. Thus, the formation of

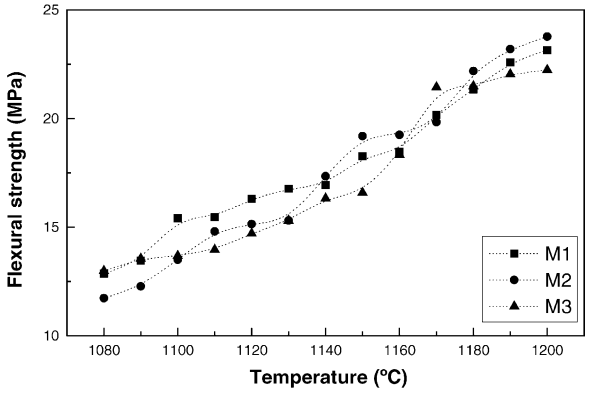

Fig. 8. Flexural strength as a function of calcareous content and sintering temperature.

crystalline phases as gehlenite and anorthite occurs to a great extent at the expense of the metakaolinite. The series of reactions with the formation of small liquid phase volume, as expected, resulted in the body having high open porosity. Also, the linear shrinkage and water absorption of the sintered bodies are practically constant within a wide firing temperature range.

We can note that the optimum firing temperature range for the ceramic formulation M1 (12 wt.% calcareous) was from 1080 to 1130 °C with linear shrinkage of 2.02–2.14%. For the ceramic formulation M2 (15 wt.% calcareous), it was from 1080 to 1140 °C with linear shrinkage of 1.96–2.06%. While that the ceramic formulation M3 (18 wt.% calcareous) presented the optimum firing temperature range from 1080 to 1160 °C with linear shrinkage of 1.89–2.03%.

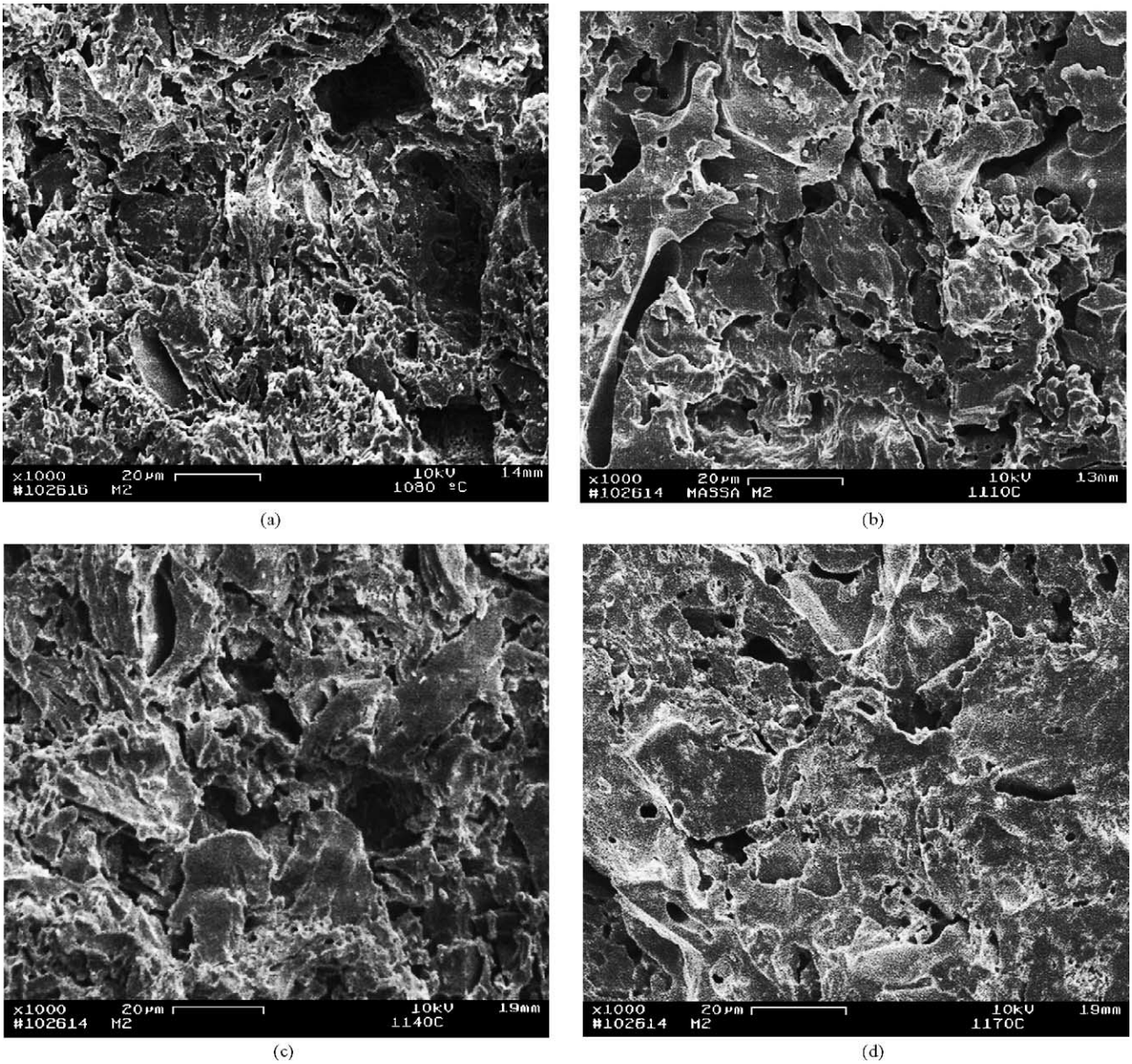

Fig. 9. SEM micrographs of the sintered specimens (formulation M2): (a) 1080 °C; (b) 1110 °C; (c) 1140 °C; and (d) 1170 °C.

The higher amount of calcareous lead to the increase of the firing range is observed. Moreover, the linear shrinkage values for all formulations are within the limits for industrial production. Water absorption (wa) is the parameter, which according to NBR 13818, defines the class to which any tile product belongs. As shown in Fig. 7(a)–(c), all the bodies presented values above 10%, indicating their conformity to NBR 13818 normative class BIII (porous wall tile).

The flexural strength of the fired bodies for all formulations as a function of the sintering temperature is shown in Fig. 8. The mechanical behaviour is quite correlated to all the others studied parameters. The flexural strength of the specimens tends to decrease as the calcareous content increases up to 18 wt.%. This is mainly attributed to the gradual modification in the level of water absorption (open porosity) of the specimens due to the evolution of more CO_2 to outside of the structure. The effect of the temperature was to increase the flexural strength by means of densification. This behaviour is due the progressive formation of calcium based crystalline phases (calcium silicates) of higher mechanical strength [12]. The wall tile bodies (thickness < 7.5 mm) with high porosity (wa $> 10\%$) at the maximum firing temperature should have values of flexural strength higher than 15 MPa, according to NBR 13818 Brazilian standard. As shown in Fig. 8, the fired bodies presented values of flexural strength in conformity to wall tiles for firing temperatures from 1100 °C (M1), 1120 °C (M2), and 1130 °C (M3).

Fig. 9 shows the microstructure of the ceramic bodies (formulation M2) sintered at various temperatures. SEM micrographs, taken at increasing firing temperatures, show the typical sequence of enhanced densification with increasing temperature, characteristic of all studied formulations in this work. As can be observed, the higher porosity connected with dense zones is cleary visible at 1080 °C (Fig. 9(a)) and at 1110 °C (Fig. 9(b)), resulting from carbonate decomposition with evolution of CO_2. At 1140 °C (Fig. 9(c)), the porosity starts to reduce. At 1170 °C (Fig. 9(d)), the bodies presented advanced sintering stage, in which, the appearance of nearly spherical isolated pores can be observed. In this state, the open porosity has been reduced and starts to negatively influence to dimensional stability of the porous wall tiles with the increase of the linear shrinkage (see Fig. 7).

X-ray diffraction patterns of the ceramic bodies (formulation M2) sintered between 1080 and 1160 °C are shown in Fig. 10. The increase of the sintering temperature for fast-firing wall tile (monoporosa) formulations exceeds the energy threshold of the reactivity of materials. As a consequence, a series of physical–chemical transformations occurred that lead to the formation of new phases and the disappearance of others [13–15]. At 1080 °C, the present phases are quartz (SiO_2), hematite (Fe_3O_4), gehlenite ($2CaO{\cdot}Al_2O_3{\cdot}SiO_2$), anorthite ($CaO{\cdot}Al_2O_3{\cdot}2SiO_2$), and primary mullite. It can be observed that the characteristic peaks (Fig. 3) of kaolinite, gibbsite, calcite, dolomite, and goethite

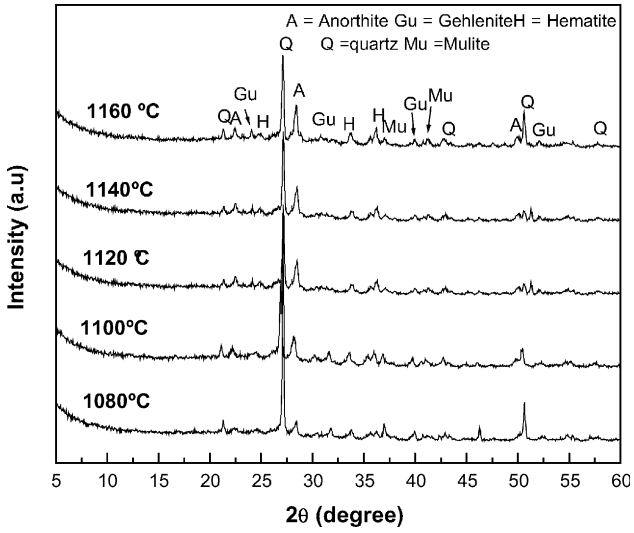

Fig. 10. X-ray diffraction patterns for the formulation M2 sintered at various temperatures.

have disappeared. The quartz peaks remain. When the temperature is increased to 1160 °C, the anorthite and hematite peak intensities begin to increase and quartz peak intensities begin to decrease. In the firing process of carbonates bearing wall tile compositions, the preferential sequence of the reactions is given by [16,17]: metakaolinite–gehlenite–anorthite. The metakaolinite was formed from kaolinite by the removal of the hydroxyl groups of the silicate lattice above 450 °C [18]. Firstly, the gehlenite is crystallised as a metastable intermediate phase from metakaolinite and calcium oxide. Later, anorthite is formed from gehlenite, which is combined with the silica and alumina rich phases due to the metakaolinite structure break, and the remaining fine quartz. The hematite appears due to the presence of a moderate iron level (Table 2) in the starting clay powder, which characterizes the studied formulations as red wall tile. The structural iron is present in the kaolinitic clays from Campos-RJ as Fe^{3+} [19]. According to the literature [17], the structural iron favours the structural

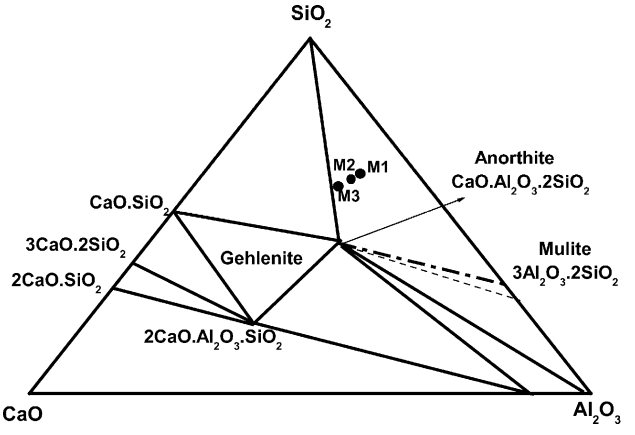

Fig. 11. Formulations plotted in the ternary phase diagram of SiO_2–Al_2O_3–CaO system.

transformations of metakaolinite to gehlenite and then to anorthite. The formulations were represented in the ternary phase diagram SiO_2–Al_2O_3–CaO [16], as shown in Fig. 11. As can be been, our formulations points are all within the triangle of compatibility quartz–anorthite–mullite (i.e., SiO_2–$CaO{\cdot}Al_2O_3{\cdot}2SiO_2$–$3Al_2O_3{\cdot}2SiO_2$). In addition, according to this phase diagram, none of the formulations show gehlenite as a stable phase, although all of them contain gehlenite as observed in Fig. 10. This demonstrates cleary that the fast-firing process used in this work does not reach the equilibrium.

4. Conclusions

The following conclusions may be drawn from the experimental results and their discussion. It has been established that the red wall tile produced by dry process presented granules with an adequate granule-size distribution and good flowability characteristics. The calcareous content and maximum firing temperature affect remarkably the tendency to the formation of calcium silicate phases such as gehlenite and anorthite. In addition, these phases play an important role in the densification of fired wall tile bodies.

The main effects of the increase of the calcareous content were to increase of the water absorption and the decrease of the linear shrinkage. It was also found that the addition of calcareous retards the densification process. The microstructure is characterized by a high porosity resulting from carbonates decomposition.

The fired bodies presented, for all formulations, good dimensional stability (low firing shrinkage) for a wide temperature range and high porosity. In addition, the studied formulations lead to ceramic tiles (class BIII) that possess the specified requirements in the Brazilian tile standard only if sintered above 1100 °C (M1), 1120 °C (M2), and 1130 °C (M3).

Acknowledgements

The authors would like to thank CAPES and CNPq (process: 551478/2002-0) for financial support to this work.

References

[1] F.H. Norton, Introduction to Ceramic Technology, Edgard Blücher, Brazil, 1973.
[2] G.J. Ghorra, Theory of fast firing, Ceram. Eng. Sci. Proc. 14 (1–2) (1993) 77–115.
[3] A. Escardino, J. García-Ten, M.C. García, M. Vicent, Descomposición de carbonatos en piezas de revestimiento poroso durante la cocción, Influencia de la temperatura, Proceedings of the QUALICER, 2000, pp. 27–29.
[4] G. Sezzi, Worldwide consumption and production of ceramic tiles, Ceram. World Rev. 48 (2002) 48–55.
[5] M.L. Oliveira, As exportações Brasileiras de produtos cerâmicos para revestimentos no período de 1980–2001, Cerâm. Ind. 7 (5) (2002) 29–39.
[6] S.J.G. Sousa, Master Thesis, in: UENF-CCT, Campos dos Goytacazes-RJ, Brazil, 2003.
[7] JCPDS, ICCD (1995).
[8] G. Nassetti, C. Palmonari, Dry fine grinding and granulation vs. wet grinding and spray drying in the preparation of a redware mix for fast-single-fired vitrified tile, Ceram. Eng. Sci. Proc. 14 (1993) 15–24.
[9] R.T. Zauberas, H.G. Riella, Defeitos de queima causados pelo quartzo em monoporosa, Cerâm. Ind. 6 (2) (2001) 40–45.
[10] A.P.N. Oliveira, Tecnologia de fabricação de revestimentos cerâmicos, Cerâm. Ind. 5 (6) (2000) 37–47.
[11] A. Escardino, Single-fired ceramic wall tile manufacture, Tile Brick Int. 9 (1) (1993) 14–19.
[12] A.A.A. Khalil, S.A. El-korashy, Firing characteristics of Sinai calcareous clays, Ceram. Int. 15 (1989) 297–303.
[13] T. Peters, R. Iberg, Mineralogical changes during firing of calcium rich brick clays, Am. Ceram. Soc. Bull. 57 (1978) 503.
[14] F.G. García, V.R. Acosta, G.G. Ramos, M.G. Rodríguez, Firing transformations of mixtures of clays containing illite, kaolinite and calcium carbonate used by ornamental tile industries, Appl. Clay Sci. 5 (1990) 361–375.
[15] A. Mergen, V.Z. Aslanoglu, Low-temperature fabrication of anorthite ceramics from kaolinite and calcium carbonate with boron oxide addition, Ceram. Int. 29 (2003) 667–670.
[16] M.M. Jórdan, T. Sanfeliu, C. De La Fuente, Firing transformations of tertiary clays used in the manufacturing of ceramic tile bodies, Appl. Clay Sci. 20 (2001) 87–95.
[17] K. Traoré, T.S. Kabré, P. Blanchart, Gehlenite and anorthite crystallisation from kaolinite and calcite mix, Ceram. Int. 29 (2003) 377–383.
[18] C.Y. Chen, G.S. Lan, W.H. Tuan, Microstructural evolution of mullite during the sintering of kaolin powder compacts, Ceram. Int. 26 (2000) 715–720.
[19] R.S.T. Manhães, L.T. Auler, M.S. Sthel, J. Alexandre, M.S.O. Massunaga, J.G. Carrió, D.R. Santos, E.C. Silva, A. Garcia-Quiroz, H. Vargas, Soil characterization using X-ray diffraction, photoacoustic spectroscopy and electron paramagnetic resonance, Appl. Clay Sci. 21 (2002) 303–311.